Stem Cell Research (2015) 14, 307–322

Available online at www.sciencedirect.com

ScienceDirect

www.elsevier.com/locate/scr

High-level *Gpr56* expression is dispensable for the maintenance and function of hematopoietic stem and progenitor cells in mice

Tata Nageswara Rao[a,b,c,d], Jonathan Marks-Bluth[e,f], Jessica Sullivan[a,b,c,d], Manoj K. Gupta[c,d], Vashe Chandrakanthan[e,f], Simon R. Fitch[g,h], Katrin Ottersbach[g,h], Young C. Jang[a,b,c,d], Xianhua Piao[i], Rohit N. Kulkarni[c,d], Thomas Serwold[c,d], John E. Pimanda[e,f], Amy J. Wagers[a,b,c,d,*]

[a] *Howard Hughes Medical Institute, USA*
[b] *Department of Stem Cell and Regenerative Biology, Harvard Stem Cell Institute, Harvard University, Cambridge, MA, USA*
[c] *Joslin Diabetes Center, Boston, MA 02215, USA*
[d] *Harvard Medical School, Boston, MA 02215, USA*
[e] *Lowy Cancer Research Centre, University of New South Wales, Sydney, NSW 2052, Australia*
[f] *Prince of Wales Clinical School, University of New South Wales, Sydney, NSW 2052, Australia*
[g] *Department of Haematology, Cambridge Institute for Medical Research University of Cambridge, Cambridge CB2 0XY, UK*
[h] *Wellcome Trust — Medical Research Council Stem Cell Institute, University of Cambridge, Cambridge CB2 0XY, UK*
[i] *Division of Newborn Medicine, Boston Children's Hospital, Harvard Medical School, MA, USA*

Received 13 November 2014; received in revised form 4 February 2015; accepted 6 February 2015
Available online 18 February 2015

Abstract
Blood formation by hematopoietic stem cells (HSCs) is regulated by a still incompletely defined network of general and HSC-specific regulators. In this study, we analyzed the role of G-protein coupled receptor 56 (*Gpr56*) as a candidate HSC regulator based on its differential expression in quiescent relative to proliferating HSCs and its common targeting by core HSC regulators. Detailed expression analysis revealed that *Gpr56* is abundantly expressed by HSPCs during definitive hematopoiesis in the embryo and in the adult bone marrow, but its levels are reduced substantially as HSPCs differentiate. However, despite enriched expression in HSPCs, *Gpr56*-deficiency did not impair HSPC maintenance or function during steady-state or myeloablative stress-induced hematopoiesis. *Gpr56*-deficient HSCs also responded normally to physiological and pharmacological mobilization signals, despite the reported role of this GPCR as a regulator of cell adhesion and migration in neuronal cells. Moreover, *Gpr56*-deficient bone marrow engrafted with equivalent efficiency as wild-type HSCs in primary recipients; however, their reconstituting ability was reduced when subjected to

Abbreviations: BMT, bone marrow transplantation; BFFP, bilateral frontoparietal polymicrogyria; G-CSF, granulocyte colony stimulating factor; GPR56, G-protein coupled receptor 56; GPCRs, G-protein coupled receptors; HSCs, Hematopoietic stem cells; HSPCs, Hematopoietic stem and progenitor cells; 5-FU, 5-Fluoro uracil.

* Corresponding author at: Joslin Diabetes Center, One Joslin Place, Boston, MA 02215, USA; Fax: +1 617 309 2593.
E-mail address: amy_wagers@harvard.edu (A.J. Wagers).

http://dx.doi.org/10.1016/j.scr.2015.02.001

serial transplantation. These data indicate that although GPR56 is abundantly and selectively expressed by primitive HSPCs, its high level expression is largely dispensable for steady-state and regenerative hematopoiesis.

Introduction

Hematopoietic stem cells (HSCs) are the only adult stem cells that can sustain lifelong blood cell production through their self-renewal and differentiation capacity. During embryonic and adult hematopoiesis, HSC homeostasis is dynamically regulated by facultative actions of cell-intrinsic and extrinsic regulators (Orkin and Zon, 2008; Wilson et al., 2010). Recent studies have identified several transcription factors as master regulators of HSC homeostasis, including *Runx1*, *Evi1*, *Gata2*, *Scl*, *Erg*, *Lyl1*, *Lmo2*, among others (Wilson et al., 2010; Ling et al., 2004; Beck et al., 2013). In addition, HSC functional properties and transcriptional programs are modulated by extrinsic factors (including, cytokines, chemokines, growth factors, and extracellular matrix proteins), which act through HSC-expressed cell surface receptors (Wang and Wagers, 2011; Ehninger and Trumpp, 2011; Levesque and Winkler, 2011). In adult bone marrow, HSCs reside in a specialized microenvironment, called the stem cell 'niche'. HSCs continuously communicate with their niche, and depend on niche-derived signals to maintain their survival, self-renewal, retention, and differentiation capacity.

Over the last decade, several studies employing genome wide transcriptional profiling analysis have revealed a unique HSC transcriptional signature and suggested that genes specifically and highly expressed in HSCs may determine HSC functional properties (Wilson et al., 2010; Ramalho-Santos et al., 2002; Gazit et al., 2013; Forsberg et al., 2010; Venezia et al., 2004; Ivanova et al., 2002) and can even specify HSC fate from more mature hematopoietic cells (Riddell et al., 2014). Although such studies have focused largely on transcriptional regulators of HSCs, it is clear that cell surface receptors can play an equally important role in the maintenance and regenerative function of stem cells by translating signals from extracellular ligands into cell physiological changes (Laird et al., 2008). G-protein coupled receptors (GPCRs) constitute one of the largest and most diverse families of membrane proteins and mediate many biological functions through 'outside in' signaling between the cell and its microenvironments (Venkatakrishnan et al., 2013). Yet, despite their functional significance in numerous cell types, few GPCRs have been investigated for their role in the regulation of HSCs. For this reason, we sought to identify the candidate HSC specific cell surface receptors by analysis of published gene expression data sets (Wilson et al., 2010; Venezia et al., 2004). From these studies, G-protein coupled receptor 56 (*Gpr56*) emerged as a highly expressed HSC-specific cell surface receptor that was present at increased levels in quiescent relative to proliferating HSCs and targeted by core HSC regulators.

GPR56 is a member of the adhesion type GPCR family (Langenhan et al., 2013), and has been implicated in regulating cell proliferation, survival, adhesion, and migration of various cell types (Iguchi et al., 2008; Luo et al., 2011a), although its physiological role in hematopoiesis is largely unexplored. In humans, mutations of *GPR56* have been linked to defects in the organization of the cerebral cortex in the brain, leading to a disorder known as bilateral frontoparietal polymicrogyria (BFPP) (Piao et al., 2004). Due to its abnormal expression levels in various cancers, GPR56 is also predicted as a tumor suppressor (Shashidhar et al., 2005). This functional versatility in various cell types, and the predominant expression pattern of GPR56 in quiescent HSCs, led us to hypothesize that this adhesion type receptor might play a critical role in regulating HSCs.

In this study, we analyzed HSC development and hematopoietic function in gene-modified mice deficient for *Gpr56*. These studies revealed that a high level of expression of *Gpr56* is largely dispensable for the development, maintenance, and differentiation of adult hematopoietic stem and progenitor cells (HSPCs) during both steady-state and myeloablative stress-induced hematopoiesis. These data suggest that low levels of GPR56 or compensatory functions of related GPCRs are sufficient to support most hematopoietic functions and raise questions regarding previously reported defects in the maintenance and function of adult hematopoietic stem and progenitor cells in *Gpr56*-deficient mice (Saito et al., 2013).

Materials and methods

Mice

Gpr56-deficient mice (B6N.129S5-*Gpr56*^{tm1Lex}/Mmcd) were generated by Genentech (South San Francisco, CA, USA), and have been reported previously (Li et al., 2008; Koirala et al., 2009; Wu et al., 2013). Genomic modification of Gpr56 alleles was verified by genotyping PCR using tail tip DNA. The following primers were used with an annealing temperature of 58 °C to identify the WT (639 bp) and *Gpr56*-deficient (369 bp) alleles: DNA085-5 5′-CGAGAAGACTTCCGCTTCTG-3′; DNA085-14 5′-AAAGTAGCTAAGATGCTCTCC-3′; Neo3a 5′-GCAGCGCATCGCCTTCTATC-3′. Wild-type littermates from heterozygous breeders were used as controls. While prior studies reported an absence of functional GPR56 protein in homozygous *Gpr56*-deficient mice (Saito et al., 2013; Li et al., 2008; Koirala et al., 2009; Wu et al., 2013), our analysis by Western blot and flow cytometry suggests residual protein expression in multiple cellular compartments, including the brain, liver and hematopoietic system (see Figs. 2B and S2B–E). B6.SJLPtprca Pep3b/BoyJ (CD45.1) mice were purchased from The Jackson Laboratory (www.jax.org). All experiments involving mice were reviewed and approved by the Institutional Animal Care and Use Committee (IACUC) of Joslin Diabetes Center and Harvard University.

In situ hybridization

Digoxigenin-labeled RNA probes were hybridized using the Ventana Discovery platform (Tucson, AZ). Data can be accessed at http://www.emouseatlas.org/.

Flow cytometry

Total bone marrow (BM), spleen, thymus and peripheral blood (PB) were harvested from age- and sex-matched mice, as indicated. BM cells were harvested from long bones (2 tibias and 2 femurs) by flushing with 25G needle using staining media (Dulbecco's PBS + 5% FCS), resuspended, and filtered through a 70 μm cell strainer. BM and splenocytes were subjected to red blood cell lysis (except when analyzing erythrocytes) using ACK lysis buffer (Lonza). To identify HSPCs, cells were stained with biotinylated lineage marker mix (Lin: anti-CD3e (17-A2), anti-CD4 (L3T4), anti-CD8 (53–6.72), anti-B220 (RA3-6B2), anti-TER-119, anti-Gr-1 (RB6-8C5), anti-Mac-1 (M1/70), followed by Streptavidin PE-Texas Red. Cells were further stained with APC-anti-c-Kit (2B8), PE-anti-CD150 (TC15-12F12.2), BioLegend), PECy7-anti-Sca-1 (E13-161.7), FITC-anti-CD34 (RAM34), FITC-anti-CD48 (HM48-1) (eBiosciences); PE-anti-Flt3 (A2F10.1), PE-FcγRII/III (2.4G2) (BD). BM myeloid progenitor subsets were identified as follows: common myeloid progenitors (CMP, $Lin^-Sca1^-cKit^+CD34^+Fc\gamma RII/III^{med}$), granulocyte monocyte progenitors (GMPs, $Lin^-Sca1^-cKit^+CD34^+Fc\gamma RII/III^+$), and megakaryocyte erythrocyte progenitors (MEPs, $Lin^-Sca1^-cKit^+CD34^-Fc\gamma RII/III^{low}$). Common lymphoid progenitors (CLPs; $Lin^-CD127^+Flt3^+$) were identified using Lin mix, PECy7-anti-CD127 (A7R34) (eBiosciences), and PE-anti-Flt3 (A2F10.1) antibodies. BM and splenic erythrocyte progenitors, BM megakaryocyte progenitors, and B-cell progenitor subsets were identified as previously described (Schepers et al., 2012). For analysis of immature thymic subsets, Lin mix, APC-anti-c-Kit (2B8), PECy7-anti-CD25 (M-A251) (BD) were used. Thymocyte differentiation was studied using CD4 and CD8 staining. Mature B cells, T cells, and myeloid cells were identified using $B220^+$, $CD3^+$, and $CD11b^+$ $Gr1^+$ staining, respectively. Cell surface GPR56 expression on BM HSPCs was assessed by using anti-human GPR56 antibody (clone: CG4, BioLegend). SYTOX-Blue (Invitrogen) was used to exclude dead cells during FACS analysis. Stained cells were analyzed on LSRII flow cytometer, and cell sorting was done on a FACS Aria II (BD). Data were analyzed by using FACS Diva software (BD) or FlowJo software (Tree Star). HSPCs from the AGM were identified by staining with CD41-Brilliant Violet 421 (Biolegend; clone MWReg30), CD34-FITC (BD Bioscience; clone RAM34), CD45-PE (eBiosciences; clone 30-F11), and cKit-APC (eBiosciences; clone 2B8). AGM sorts were performed on an influx cytometer.

Peripheral blood (PB) analysis and differential count

PB was collected from the tail vein of adult mice into EDTA-coated tubes (BD), and differential blood counts were determined using a Hemavet 950 (Drew Scientific).

RT-PCR

For analysis of Col3A and *Gpr56* expressions in the AGM, tissues were dissociated and RNA isolated, reverse transcribed and amplified according to the methods described in (Fitch et al., 2012), using the following primer sets: MmGpr56, JP593F 5′-ATCAGCCAGCAGTTACAG-3′ and JP593R 5′-GAAGCAACAGCGAGTATG-3′; MmCol3a, JP596F 5′-GAATCT GTGAATCATGTCCAACTG-3′ and JP596R 5′-CCACCCATTCCTC CCACTC-3′; SDHA_F 5′-TTG CTA CTG GGG GCT ACG GGC-3′ and SDHA_R 5′-TGA CCA TGG CTG TGC CGT CC-3′; B-actin_F 5′-TCC TGG CCT CAC TGT CCA-3′ and B-actin_R 5′-GTC CGC CTA GAA GCA CTT GC-3′. For analysis of *Gpr56* expression in adult cell populations, total RNA was extracted from the indicated FACS-purified cells by RNeasy micro kit following manufacturer's instructions (Qiagen) and reverse transcribed into cDNA using SuperScript Vilo cDNA Synthesis kit (Invitrogen). Quantitative PCR was performed with an AV7900 PCR system using Taqman Gene Expression master mix kit (Applied Biosystems). Taqman gene expression primer sets were used to quantify the *Gpr56* (Mm00817704_m1) and *β-actin* (Mm00607939_s1) gene expression levels. The expression levels of the *β-actin* house-keeping gene were used to normalize *Gpr56* expression in indicated subsets.

Western blot analysis

Total protein lysates from the FACS-sorted BM HSPCs, liver and embryonic brain (embryonic day (E) 14.5) were subjected to standard Western blot analysis. Total protein was loaded onto 4–16% gradient SDS-PAGE gel and transferred onto a PVDF membrane. Mouse anti-human GPR56 monoclonal antibody (1:500 dilution, Millipore catalog #MABN310 (Jeong et al., 2012)) was used to detect GPR56 protein. β-Actin (Santa Cruz) was used as loading control.

Colony-forming unit cell assay (CFU-C)

BM and PB cells were mixed with 300 μL of IMDM and 4 mL of defined semisolid methylcellulose medium (Methocult GF3434 medium, StemCellTechnologies). Cells were then cultured in triplicate in 6-well plate with 1.1 mL/plate at a density of 1×10^4 cells for BM and 1×10^5 cells for PB. The total number of colonies was counted at day 10 under an inverted microscope.

Cell cycle analysis and apoptosis assay

BM and thymocyte cell cycle status was determined using Ki67/Hoechst staining. Cells were first stained with surface antibodies to identify indicated subsets and then fixed in Cytofix buffer for 20 min, washed and permeabilized using Cytofix/perm buffer (BD) before staining with Ki67-FITC (B56) antibody (BD) for 30 min at 4 °C. Cells were washed once with permeabilization buffer after staining and incubated with Hoechst dye (20 μg/mL) and analyzed by BD LSR II flow cytometer. To assess the in vivo cell proliferation rate of thymocytes, 1 mg of BrdU was injected (i.p.) and mice were sacrificed 5 h later (short-term pulse). BrdU incorporation was detected with the BrdU flow kit following the manufacturer's instructions (BD Biosciences). To assess survival rate, mononuclear cells (1×10^6) from BM

or thymus were surface stained with the appropriate antibodies to identify indicated subsets. Cells were washed with PBS and then resuspended in 100 μL of Annexin V binding buffer (BD) and incubated with AnnexinV and 7-AAD (BD Pharmingen) for 15 min at room temperature. Cells were resuspended in additional 400 μL of Annexin V binding buffer and analyzed immediately using a BD LSR II flow cytometer.

Bone marrow (BM) reconstitution assays

For competitive repopulation experiments, total BM cells (1×10^6) from either WT control littermates or *Gpr56*-deficient mice (CD45.2) were mixed with equal number (1:1) of recipient type cells (CD45.1) and transplanted into lethally irradiated (950 rads) B6SJL Ptprca Pep3b/BoyJ (CD45.1) congenic recipients by lateral tail vein injections (in 200 μL PBS/mouse). At the indicated time points post-transplantation, recipient mouse PB was collected, erythrocytes were depleted with ACK buffer (Lonza), and the remaining leukocytes were stained with anti-mouse CD45.2, CD45.1, CD3, B220, Gr-1, and CD11b antibodies. Stained cells were analyzed by FACS LSRII (BD).

5-FU treatment

5-Fluorouracil (5-FU, Sigma) was administered to mice intravenously at a dose of 150 mg/kg. Hematopoietic recovery was monitored by differential blood cell counts using the Hemavet 950 (Drew Scientific), at indicated time points. For survival assay, 5-FU was administered intraperitoneally at a dose of 150 mg/kg weekly for a total of 3 weeks and the survival of individual mice was monitored daily.

In vitro transwell migration assay

In vitro migration of HSPCs was performed using transwells (6.5 mm diameter inserts; 5 μm pore size; Corning). FACS-purified HSPCs were loaded onto transwell inserts (10^5 cells/well in 100 μL of the medium). The lower chambers contained 600 μL of RPMI medium supplemented with 10% FCS and with SDF-1 (100 ng/mL) or without SDF-1 (R&D systems). Cells were incubated for 4 h at 37 °C and 5% CO_2. Migrating cells from the lower chambers were collected and counted by FACS with normalization using CountBright Absolute counting beads (Invitrogen). The percentage of migrated cells was calculated by dividing the absolute number of migrated cells by the input cell number.

In vivo lodging assay

For in vivo lodging assays, FACS-isolated Lin^-Kit^+ cells from WT and KO mice were labeled with 4 μM of PKH67 (Sigma) vital fluorescent dye and intravenously infused into the non-irradiated wild-type littermates. Sixteen hours post-transplantation, BM and spleen were harvested from the recipient mice and analyzed for the labeled lodged cells by FACS using FITC channel.

G-CSF treatment and mobilization assay

Cytokine induced mobilization of HSPCs was performed by daily subcutaneous administration of G-CSF (Filgrastim, Amgen), 300 μg/kg in 200 μL of PBS for five consecutive days, as previously described (Gazit et al., 2013; Neben et al., 1993). Control mice received PBS only. PB and spleen were collected on the sixth day and analyzed for HSPC (LSK) frequency by FACS.

Statistics

Statistical significance was determined with Student's *t*-test using GraphPad Prism Software Version 6.0. For the Kaplan–Meier analysis of survival curves, a log-rank non-parametric test (Mantel–Cox) was performed. *p*-Values are denoted with $^*(p < 0.05)$; $^{**}(p < 0.01)$; and *n.s.* (not significant).

Results

Gpr56 is abundantly expressed in HSCs during definitive hematopoiesis in the mouse embryo and is a heptad target

Recent studies have postulated that genes specifically expressed in HSCs relative to their more differentiated progeny may play an important role in fine-tuning HSC properties (Gazit et al., 2013; Chambers et al., 2007). To identify candidate HSC-specific regulators we made use of published data sets that identified genes uniquely expressed by quiescent, versus proliferating, HSCs (Q-group, (11)) in combination with a proximal promoter-based analysis of genes that are bound by seven key hematopoietic transcription factors (*Scl*, *Gata2*, *Runx1*, *Erg*, *Fli1*, *Lyl1*, and *Lmo2*) (Wilson et al., 2010), which together are referred to as Heptad targets (Fig. 1A). Comparative analysis of these gene sets identified a total of 81 transcripts that showed enriched expression in quiescent HSCs and contained Heptad binding sites in their upstream regions.

Although much attention has been focused on transcriptional regulators of HSCs, it is clear that surface receptors play an equally important role. Based on the rationale that cell quiescence is likely to be mediated by niche interactions (Wang and Wagers, 2011), we further filtered this gene list for cell surface receptors, identifying eight receptors (*Gpr56*, *Adrb2*, *Ifnar2*, *Vldlr*, *Fgfr1*, *Igf1r*, *Il1r1* and *Csf2rb* (*Il3rBC*)) (Supplemental Table 1) specifically enriched in quiescent HSCs and containing Heptad binding sites in their proximal regions. Of these eight, we focused on *Gpr56* for further investigation because of its unknown physiological function, the availability of *Gpr56*-deficient mice, and because prior studies implicated this receptor in the regulation of adhesion and migration of neuronal progenitors and malignant cells (Li et al., 2008; Koirala et al., 2009; Wu et al., 2013). Interestingly, a study published during the preparation of this manuscript reported a disruption of HSC localization, cycling and in vivo repopulating capacity in mice deficient for *Gpr56* expression (Saito et al., 2013).

To determine the role of *Gpr56* during the early stages of hematopoietic development, we examined its expression during definitive hematopoiesis in the aorta-gonad-mesonephros

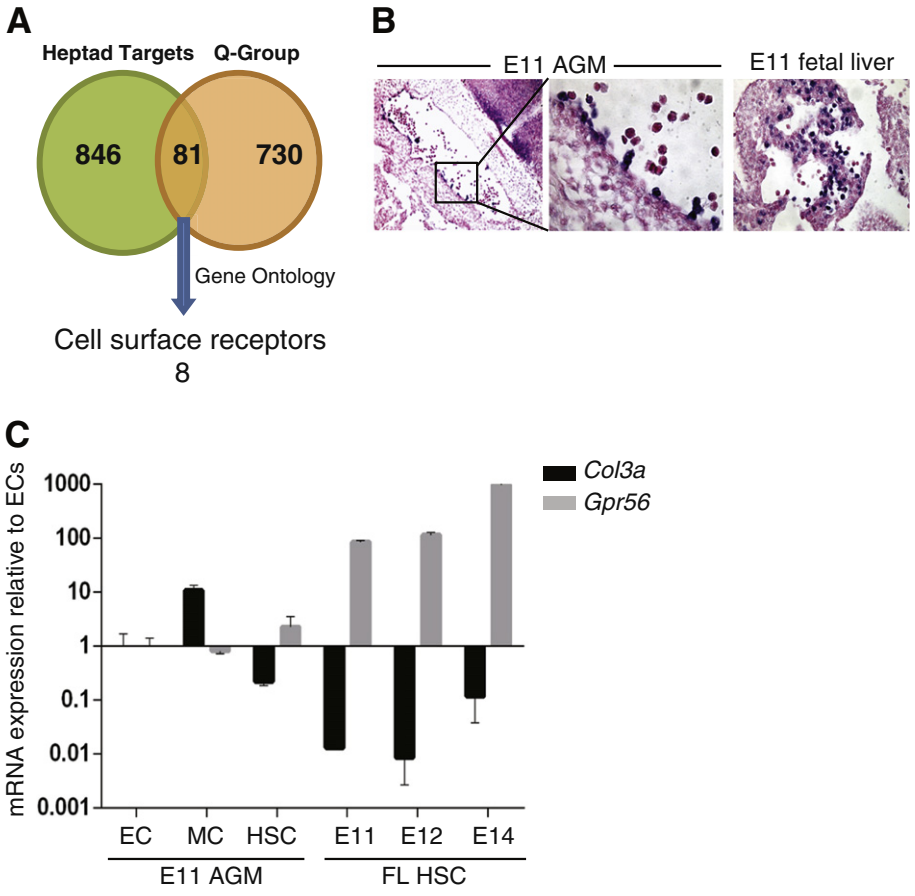

Figure 1 *Gpr56* is expressed in HSCs during definitive hematopoiesis in the mouse embryo and is a Heptad target. (A). Venn diagram showing the overlap between two data sets, one from ChIP-Seq data in HPC7 progenitor cells containing genes with combinatorial binding regions bound by seven key HSC transcription factors (*Scl*, *Gata2*, *Runx1*, *Erg*, *Fli1*, *Lyl1* and *Lmo2*; Heptad targets) (Wilson et al., 2010) and the other comparing gene expression in quiescent versus proliferating HSCs (Q group) (Venezia et al., 2004). The overlap (n = 81) between these two data sets was further filtered for cell surface receptors, identifying 8 receptors (Supplemental Table S1). (B). In situ hybridization for *Gpr*56 showing transcript expression in blood clusters and adjacent endothelium in E11 AGM and in E11 FL blood cells. (C). Quantitative PCR for *Gpr*56 and its ligand *Col3a* in E11 AGM endothelial cells (EC; $CD34^+CD45^-$), E11AGM mesenchymal cells (MC; $CD34^-CD45^-cKit^-$), E11 AGM hematopoietic stem cells (HSC; $CD34^+CD45^+cKit^+CD41^{int}$); E11, E12 FL HSC; $CD34^+ckit^+$ and E14 FL HSC; Lin^- $CD45^+$ $CD48^-$ $CD150^+$ $EPCR^+$.

region (AGM) and fetal liver (FL) of mouse embryos. In situ hybridization revealed the expression of *Gpr*56 transcripts in emerging clusters of blood cells and adjacent endothelium in E11 AGM and in E11 FL cells in the mouse embryo (Fig. 1B). Notably, quantitative RT-PCR analysis revealed that collagen III (*Col3a*) the reported ligand of GPR56 (Luo et al., 2011a) is expressed in E11 AGM mesenchymal cells (MC; $CD34^-CD45^-cKit^-$), but not in endothelial cells (EC; $CD34^+CD45^-$), or in AGM or FL HSCs ($CD34^+CD45^+c\text{-}kit^+CD41^{int}$) (Fig. 1C). Conversely, *Gpr56* was absent in E11 AGM mesenchymal cells and endothelial cells, but was significantly elevated in HSCs during the developmental transition from E11 AGM to E14 fetal liver stages (Fig. 1C), suggesting a possible role for GPR56 signaling in the regulation of HSCs during early definitive hematopoiesis. Consistent with this, a recent study in zebrafish embryos reported a defect in HSC emergence in the caudal hematopoietic tissue upon *gpr56* knockdown by morpholino oligos (Solaimani Kartalaei et al., 2015).

Gpr56 is highly expressed in adult HSCs, but is dispensable for steady-state maintenance of adult stem and progenitor cells

We next determined the expression pattern of *Gpr56* in adult bone marrow. Consistent with prior studies (Venezia et al., 2004), quantitative RT-PCR analysis of purified HSPCs from adult wild type C57BL/6 bone marrow revealed that *Gpr56* is expressed most abundantly in primitive HSPCs, with the highest expression detected in long-term, self-renewing HSCs (LT-HSCs, $LSKCD34^-Flt3^-$) followed by short-term (ST-HSCs, $LSKCD34^+Flt3^-$) and multipotent progenitors (MPPs, $LSKCD34^+Flt3^+$) (Fig. 2A). Strikingly, *Gpr56* expression levels were progressively down-regulated in lineage-restricted lymphoid and myeloid progenitor subsets (Fig. 2A). We also analyzed *Gpr56* expression across a broad range of hematopoietic subsets, taking advantage of two publically accessible databases/web servers, ImmGen

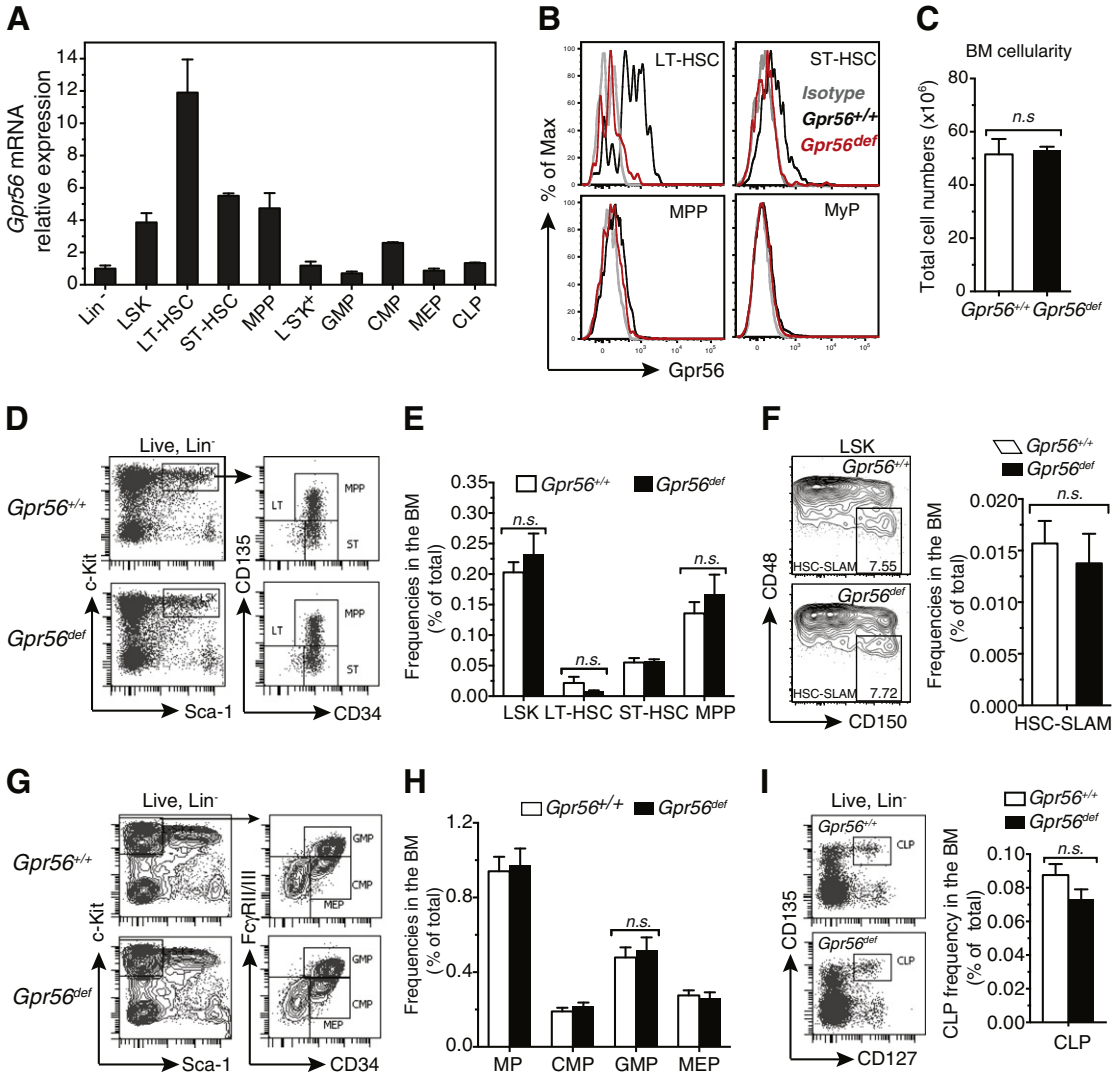

Figure 2 *Gpr56* is highly expressed in adult HSCs, but dispensable for maintaining HSPC numbers in the steady-state. (A). *Gpr56* expression was quantified by qRT-PCR analysis in the indicated FACS-purified HSPCs of WT C57BL/6 mice. Expression values in each subset were normalized to an internal control (*β-actin* gene). Data are plotted as fold-expression relative to *Gpr56* expression in lineage negative (Lin^-) cells, whose expression was arbitrarily set to one. Data represent mean ± SD, n = 4 independent samples from two independent experiments. (B). Expression of GPR56 on the cell surface of the indicated BM HSPC subsets from WT and *Gpr56*-deficient mice was determined by FACS using anti-GPR56 antibody (clone: CG4). (C). Total BM cell numbers of 8–14 week old *Gpr56*-deficient mice and WT littermates. Cell counts determined from two tibias and two femurs from each mouse (n = 8 mice per group). (D). Representative FACS plots showing the percentages of HSPC subsets (as indicated) in the BM of WT and *Gpr56*-deficient mice. $Lin^-Sca1^+ckit^+$ (LSK) cells (left plots) were further fractionated based on CD34 and CD135 expression levels into LT-HSCs ($LSKCD34^-CD135^-$), ST-HSCs ($LSKCD34^+CD135^-$), and MPPs ($LSKCD34^+CD135^+$) (right plots). (E). Bar graph indicating the frequency of indicated subsets in the whole BM of WT and *Gpr56*-deficient mice. Data represent mean ± SEM, n = 10 independent samples from 3 independent experiments. (F). Representative FACS plots showing the percentages of HSC-SLAM cells ($LSKCD48^-CD150^+$), and graph summarizing HSC-SLAM frequency in whole BM of WT and *Gpr56*-deficient mice. (G). Detection of myeloid progenitors in the BM by FACS. $Lin^-Sca\text{-}1^-c\text{-}Kit^+$ myeloid progenitors (MPs, left FACS plots) were subdivided according to CD34 and FcγRII/III expression (right FACS plots), the common myeloid progenitors (CMP, $Lin^-Sca\text{-}1^-c\text{-}Kit^+CD34^+FcγRII/III^{med}$), granulocyte monocyte progenitors (GMPs, $Lin^-Sca\text{-}1^-c\text{-}Kit^+CD34^+FcγRII/III^+$), and megakaryocyte erythrocyte progenitors (MEPs, $Lin^-Sca\text{-}1^-c\text{-}Kit^+CD34^-FcγRII/III^{low}$). (H). Frequencies of the indicated subsets in whole BM of WT and *Gpr56*-deficient mice. Data represent mean ± SEM, n = 5 independent samples from two independent experiments. (I). FACS plots and graph represent the frequency of common lymphoid progenitors (CLPs, $Lin^-CD127^+CD135^+$) in the whole BM of WT and *Gpr56*-deficient mice. Data are mean ± SEM, n = 7–10 mice from 3 independent experiments.

(https://www.immgen.org/) and HemaExplorer (http://servers.binf.ku.dk/hemaexplorer; (Bagger et al., 2012)), in which microarray based mRNA expression profiles of previously reported FACS sorted populations of immature and mature hematopoietic subsets can be visualized. Consistent with our qRT-PCR results, within these data

sets, *Gpr56* expression was most abundant in the primitive HSC fraction, when compared to any other progenitor subset in the BM or mature hematopoietic cell subset in the periphery (Supplemental Figs. S1A, B). We also noted moderate expression of *Gpr56* in megakaryocyte progenitors (MkP) in the BM, and in early thymic progenitors (Supplemental Fig. S1B). Together, these results indicate that *Gpr56* expression is tightly regulated within primitive HSPCs, and that the level of *Gpr56* expression declines sharply as HSCs undergo lineage restriction and differentiation into mature blood lineages.

These results prompted us to explore further the role of GPR56 in adult hematopoiesis. We hypothesized that if enriched expression of *Gpr56* predicted its functional activity, then we could expect to see changes in HSPCs and in steady-state hematopoiesis in *Gpr56*-deficient mice (Supplemental Fig. S2A). We thus performed FACS-immunophenotyping to assess the frequencies of specific HSPC subsets in the BM of adult *Gpr56*-deficient mice. Interestingly, although prior studies of these animals have suggested that they lack GPR56 protein entirely (Luo et al., 2011a; Saito et al., 2013; Li et al., 2008; Wu et al., 2013), our analysis using highly specific anti-GPR56 mAb (Luo et al., 2011a) revealed some residual expression in the brain, liver, and hematopoietic compartment (Supplemental Figs. S2B–D). Nonetheless, flow cytometric analysis of HSPC populations in these animals indicated a substantial reduction of GPR56 protein on the cell surface, including a >4-fold reduction of GPR56 staining of LT-HSCs from *Gpr56*-deficient BM (Fig. 2B and Supplemental Fig. S2E).

Further analysis of hematopoietic subsets in *Gpr56*-deficient mice indicated that, despite the abundant and relatively restricted expressions of this protein by primitive HSPCs, *Gpr56*-deficient mice displayed no abnormalities in steady-state hematopoiesis. Total BM cellularity and frequencies of LT-HSC ($LSKCD34^{-}CD135^{-}$), ST-HSC ($LSKCD34^{+}CD135^{-}$) and MPPs ($LSKCD34^{+}CD135^{+}$) in the BM were indistinguishable from WT control littermates (Figs. 2C–E). Likewise, further enrichment of HSCs within the LSK subset, using SLAM family receptor expression ($LKSCD150^{+}CD48^{-}$ (Kiel et al., 2005)), also revealed HSC frequencies that were unaffected by the reduction of *Gpr56* (Fig. 2F). We did observe a mild reduction in LT-HSC ($LSKCD34^{-}CD135^{-}$) frequency in *Gpr56*-deficient BM, but this reduction was not statistically significant ($p = 0.209$). A detailed analysis of lineage committed progenitors, including myeloid progenitors (MPs), common myeloid progenitors (CMPs), granulocyte monocyte progenitors (GMPs), and megakaryocyte erythrocyte progenitors (MEPs), and common lymphoid progenitors (CLPs) similarly showed frequencies indistinguishable from those in wild type BM (Figs. 2G–I and Supplemental Figs. S3A–B). B-cell progenitors were mildly decreased at the Pre-B and Pro-B stages; however, this defect was resolved at the mature B cell stage (Supplemental Figs. S3C–D).

We also performed detailed immunophenotyping and differential blood counts of mature hematopoietic lineages in the BM and PB to determine if specific lineages might be affected in *Gpr56*-deficient mice. The frequencies of mature T-cells ($CD3^{+}$), B-cells ($B220^{+}$), myeloid cells ($CD11b^{+}Gr\text{-}1^{+}$), and erythroid lineage cells in the BM and the overall PB cell counts were unchanged, indicating unaffected lymphopoiesis and myelopoiesis in mice with reduced levels of functional GPR56 (Table 1 and Supplemental Figs. S3C, E–G). Altogether, these results indicate that despite its enriched expression in primitive HSPCs, high level GPR56 is largely dispensable for steady-state HSPC maintenance and hematopoietic differentiation.

Enlarged thymuses and increased frequency of early thymic precursors in *Gpr56*-deficient mice

To further assess any effects on blood cell development in the absence of high levels of GPR56, we investigated hematopoiesis in the spleen and thymus of *Gpr56*-deficient mice. Analysis of splenic lineages revealed normal cellularity and frequencies of myeloid, B-cells and erythroid lineages (Supplemental Figs. S4A–C); however, the frequencies of $CD4^{+}$ and $CD8^{+}$ T cells were slightly but significantly reduced in *Gpr56*-deficient mice (Figs. S4D–E). We also consistently observed enlarged thymuses in *Gpr56*-deficient mice compared with age-matched littermate controls (Fig. 3A). Thymic analysis showed that *Gpr56*-deficient mice at 8–14 weeks of age exhibited significantly higher numbers of thymocytes (~1.4-fold) compared with age-matched controls (159 ± 7 for WT and 225 ± 13 for *Gpr56*-deficient mice, $p = 0.0002$) (Fig. 3B). In addition, histological analysis revealed that the thymus of *Gpr56*-deficient mice possessed

Table 1 Differential blood cell counts on peripheral blood from $Gpr56^{+/+}$ and $Gpr56^{def}$ littermates.

Parameter	$Gpr56^{+/+}$	$Gpr56^{def}$	*p*-Value
WBCs (K/μL)	9.29 ± 5.12	6.87 ± 3.78	0.20
Neutrophils (K/μL)	2.71 ± 1.91	1.56 ± 0.75	0.10
Lymphocytes (K/μL)	5.74 ± 4.09	5.03 ± 3.04	0.64
Monocytes (K/μL)	0.51 ± 0.3	0.24 ± 0.29	0.13
Eosinophils (K/μL)	0.26 ± 0.19	0.03 ± 0.03	0.06
Basophils (K/μL)	0.04 ± 0.07	0.01 ± 0.01	0.12
RBC (M/μL)	9.42 ± 1.25	9.03 ± 2.21	0.58
Hb (g/dL)	12.84 ± 1.89	12.33 ± 3.21	0.64
HCT (%)	46.65 ± 6.21	45.57 ± 12.05	0.78
MCV (fL)	49.46 ± 2.89	50.13 ± 2.58	0.58
PLT (K/μL)	766.58 ± 200.12	829.42 ± 206.48	0.43

Values shown are means ± SEM (n = 12 mice per group). WBC indicates white blood cell; RBC, red blood cell; Hb, hemoglobin; HCT hematocrit; MCV, mean corpuscular volume; and PLT, platelets. No statistically significant differences were detected.

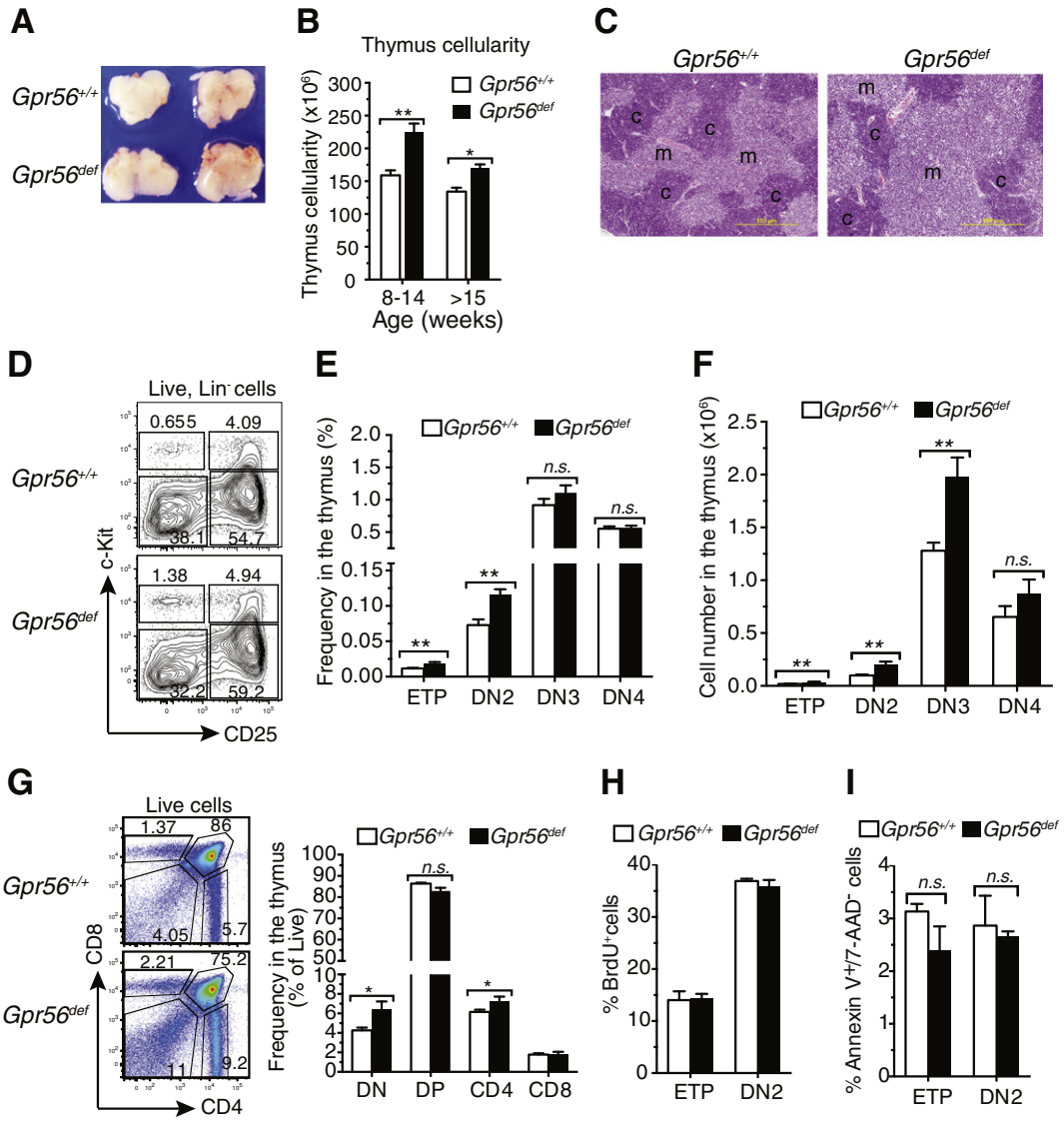

Figure 3 Enlarged thymus and increased frequency of early thymic precursors in *Gpr56*-deficient mice. (A). Representative photographs of thymuses from 10-week-old WT and *Gpr56*-deficient mice. (B). Increased thymic cellularity in *Gpr56*-deficient mice. Graph shows the absolute number of thymocytes from the indicated age group of WT or *Gpr56*-deficient mice (mean ± SEM, n = 9–12 mice). (C). Hematoxylin and eosin (H&E) staining of thymus from 12-week old WT and *Gpr56*-deficient mice (representative of n = 4 per genotype) (m: medulla; c: cortex). (D). FACS contour plots display the distribution and percentages of immature thymocyte subsets within the Lin^- fraction of thymocytes from 10-week-old WT and *Gpr56*-deficient mice. (E–F). Graphs show the frequencies (E) and absolute number of thymocytes (F) of indicated immature thymocyte subsets in the thymus (n = 12 mice per genotype, mean ± SEM). (G). Thymocytes from 10-week-old WT and *Gpr56*-deficient mice were surface stained for CD4 and CD8 to assess thymocyte differentiation. FACS plots show the distribution of DN ($CD4^-/CD8^-$), DP ($CD4^+/CD8^+$), $CD4^+$ and $CD8^+$ cells. Graphs show the percentages of indicated subsets in the thymus (n = 11 mice). (H). Mice were treated by i.p. injection of 1 mg of BrdU and sacrificed 5 h later. The data show percentage of cells with BrdU-incorporation in the indicated thymic subsets (n = 5, means ± SEM). (I). Apoptosis rates in the thymocytes from 8-week-old WT and *Gpr56*-deficient mice were determined by Annexin V/7-AAD staining. Percentages of apoptotic cells are summarized in the graph (n = 5, means ± SEM). *$p < 0.05$, **$p < 0.01$, and *n.s.* (not significant).

abnormal cortex and medullary proportions with an enlarged medullary region (Fig. 3C).

It has been reported that increased frequency of early thymic progenitors (ETP) due to increased recruitment of progenitors from the BM into the thymus could led to increased thymic cellularity (Schnell et al., 2006). Therefore, we next studied the early stages of thymocyte development to determine whether *Gpr56*-deficiency increased the ETP and CD4/CD8-double negative thymocyte subsets. Fractionation of Lin^- thymocytes using CD25 and c-Kit surface expression revealed that *Gpr56*-deficient mice have significantly higher percentages and absolute numbers of ETPs ($Lin^-CD25^-c\text{-}Kit^+$) in the thymus (Figs. 3D–F). Analysis of subsequent developmental stages showed that *Gpr56*-deficient mice also

possessed higher numbers of DN2 ($Lin^-CD25^+c\text{-}Kit^+$), DN3 ($Lin^-CD25^+c\text{-}Kit^{lo}$) and mature CD4 and CD8 single positive cell subsets (Figs. 3D–G, and data not shown).

It is possible that increased cycling or survival of early thymic precursors could account for the increased cellularity in *Gpr56*-deficient mice. Thus, to determine cellular proliferation rates, we pulsed these mice with BrdU for 5 h and analyzed the frequency of $BrdU^+$ cells; however, WT and *Gpr56*-deficient ETPs and DN2 cells showed comparable proliferation rates (Fig. 3H). Cell survival measurements using Annexin V staining likewise showed that *Gpr56*-deficient ETPs exhibited similar rates of apoptosis as their WT counter parts (Fig. 3I). Analysis of all other developmental stages, including $CD4^+$, $CD8^+$, and DP stages, also showed comparable rates of cycling and comparable frequencies of apoptotic cells between WT and *Gpr56*-deficient thymocytes (data not shown). The observed increase in the number of ETPs and DN2 cells in *Gpr56*-deficient thymuses, despite normal proliferation and survival rates, suggests that *Gpr56* deficiency may alter the intrinsic ability of *Gpr56*-deficient BM progenitors to migrate from the BM into the thymus. It is also possible that *Gpr56*-deficient thymuses may be more receptive to BM progenitor entry. Regardless, increased numbers of ETPs and DN2 cells likely account for the increased number of subsequent thymocyte stages, and hence the overall increase in thymic cellularity.

High-level GPR56 expression is largely dispensable for regulation of HSPC proliferation and survival and for reconstitution of the hematopoietic system after BM transplantation

Although detailed immunophenotyping analysis by flow cytometry suggested no reduction in HSPC content in *Gpr56*-deficient BM (Fig. 2), it is possible that homeostatic effects during development could mask defects in HSPC maintenance in *Gpr56*-deficient mice through functional compensatory mechanisms. Therefore, we next tested whether changes in cell proliferation or survival might have provided a selection advantage toward normal HSPC pool size. To directly assess the cell-cycle status of *Gpr56*-deficient HSPCs, we stained the cells with Ki-67, a proliferation marker, and Hoechst 33342 for DNA content analysis. No differences were noted in the percentages of quiescent (G0, $Ki67^-Hoechst^-$) or cycling cells (S/G2/M, $Ki67^+Hoechst^+$) in WT and *Gpr56*-deficient HSPC subsets (Figs. 4A–B). Next, we co-stained cells with Annexin V and 7-AAD and analyzed possible effects on survival by flow cytometry. The percentages of early apoptotic cells (Annexin V^+ $7\text{-}AAD^-$) among *Gpr56*-deficient LSK HSPCs cells were not significantly different from WT littermates (Fig. 4C, 6.88 ± 1.13 and 5.83 ± 0.8, for *Gpr56*-deficient and WT, respectively) ($p = 0.47$). These findings are in line with our earlier observations that phenotypic HSPCs are largely intact in *Gpr56*-deficient BM. Altogether, these results suggest that *Gpr56*-deficiency does not affect HSPC quiescence or survival in the adult mouse bone marrow during steady-state conditions.

To evaluate the hematopoietic reconstituting ability of *Gpr56*-deficient HSCs, we next performed competitive repopulation assays in which equal numbers of total BM cells ($CD45.2^+$) from WT or *Gpr56*-deficient mice were mixed at a 1:1 ratio with congenic ($CD45.1^+$) WT competitor cells and transplanted into lethally irradiated primary recipient mice (Fig. 4D). Previously, Saito et al. (2013), reported that *Gpr56*-deficient HSCs possess reduced reconstitution potential due in part to reduced homing capacity. We speculated that if GPR56 regulates HSC homing capacity we should see an alteration in hematopoietic repopulation in recipients particularly at early stages after BM transplantation; however, analysis of peripheral blood of recipient mice at 4-weeks after transplant showed no significant differences between WT and *Gpr56*-deficient donors in either the reconstitution of total hematopoietic lineages (percent $CD45.2^+$) or the repopulation of B ($B220^+$), T ($CD3^+$) and myeloid cells ($Gr1^+CD11b^+$) (Figs. 4E–H), suggesting that high level GPR56 expression is not needed for HSC homing or short-term reconstitution in primary transplant recipients. Subsequent analysis of long-term reconstitution, at 8, 12, and 20 w post-BMT, revealed that *Gpr56*-deficient donors did not differ in their ability to reconstitute B, T, and short-lived myeloid cells (a measure for intact HSC activity) in the PB or BM of primary recipients (Figs. 4E–I). Furthermore, the frequencies of donor LSK cells in the BM of primary recipient mice were also similar (80.9 ± 5.9 vs. 70.8 ± 22.5, $p = 0.41$) in the two groups (Fig. 4J).

To further assess the regenerative capacity of *Gpr56*-deficient HSCs, we performed secondary transplantation (which imposes extreme proliferative stress for HSCs) using total BM cells from primary recipients harvested 20 weeks after the primary transplant. Intriguingly, while donor B-cell and T-cell chimerism was almost identical in secondary recipients of WT and *Gpr56*-deficient marrow, donor myeloid lineage chimerism in the PB ($p = 0.001$) and the total donor cell frequency in the BM was significantly reduced ($p = 0.0027$) in secondary recipients of *Gpr56*-deficient BM (Figs. 4K–L). Analysis of the LSK compartment also showed a significant reduction of HSPC frequency (86.3 ± 11.7 for WT vs 42.2 ± 24.6 for *Gpr56*-deficient mice, $p = 0.006$) in secondary recipients of *Gpr56*-deficient BM (Fig. 4M). Taken together, these results indicate that although high levels of GPR56 appear dispensable for hematopoietic reconstitution in primary recipients, *Gpr56*-deficient HSCs can show reduced regenerative capacity when subjected to repeated proliferative stress induced by serial BM transplantation.

Gpr56-deficiency does not alter recovery from myelosuppression or impair the physiological or pharmacological mobilization of HSPCs

The defects we observed upon serial transplant of *Gpr56*-deficient BM cells suggested that reduction of GPR56 protein levels on HSPCs might impact the hematopoietic function of these cells when subjected to repeated proliferative or migratory stress. During steady-state conditions, the majority of HSCs are maintained in a quiescent state (G0) in the BM; however, during infections, and in response to irradiation or chemotoxic drugs, HSCs exit quiescence and enter the cell cycle to replenish the hematopoietic system. These cells also can be induced by such stimuli to migrate from the BM niche to seed extramedullary hematopoiesis (Wright et al., 2002). During these responses, the balance between proliferation and differentiation must be tightly controlled to sustain the

ability of HSCs to regenerate the hematopoietic system (Passegue et al., 2005).

To elucidate whether GPR56 plays any role regenerating the hematopoietic system during such conditions, we treated mice with a single dose of 5-fluorouracil (5-FU) intravenously, a cytotoxic drug that kills actively cycling cells and induces quiescent HSCs to rapidly proliferate. We monitored the kinetics of hematopoietic recovery in the peripheral blood at every fourth day for a total of 24 days after 5-FU treatment. In agreement with previous studies, we observed multi-lineage hematopoietic recovery, including white blood cells (WBC), platelets, and red blood cells (RBC), at days 16–20 after 5-FU treatment in the peripheral blood of WT mice (Figs. 5A–C). However, we found no significant differences in blood cell

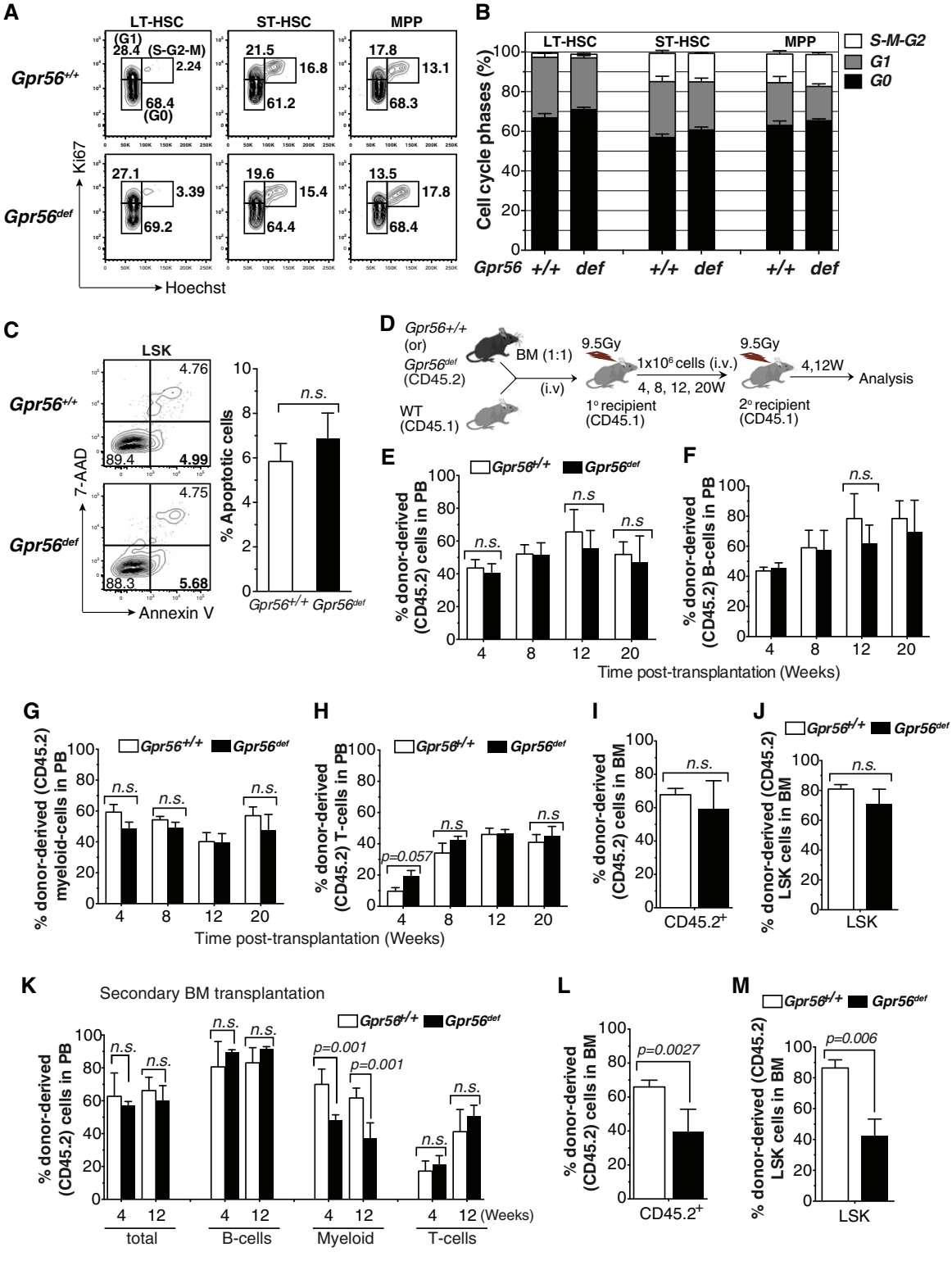

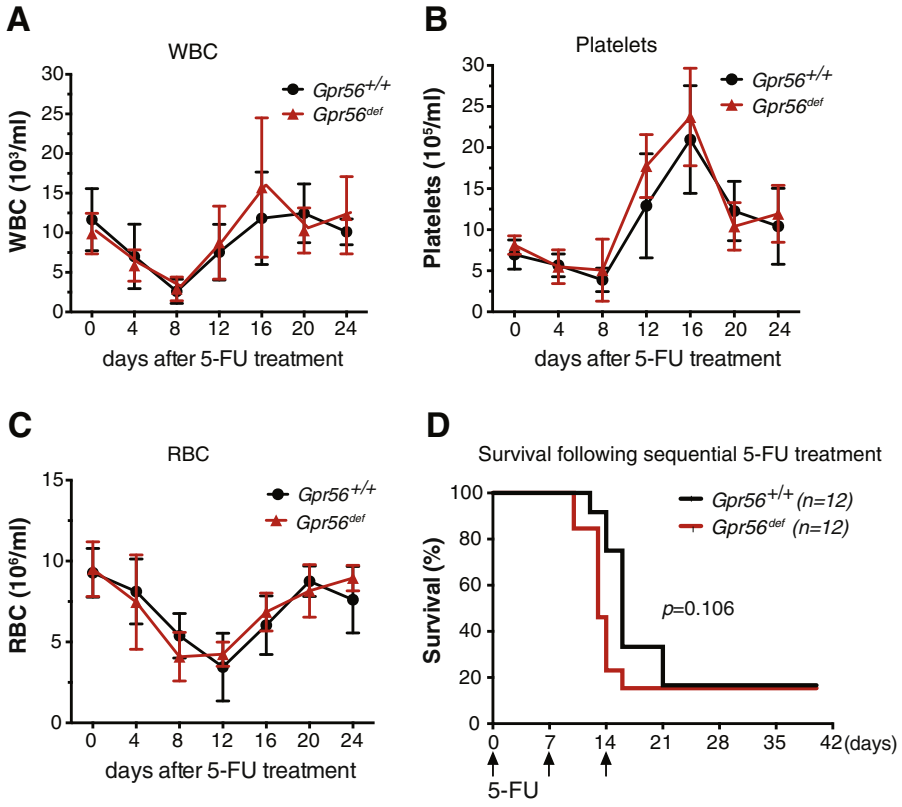

Figure 5 Normal hematopoietic recovery and survival of *Gpr56*-deficient mice after myelosuppressive treatment with 5-FU. Eight to ten week-old WT and *Gpr56*-deficient mice were intravenously injected with a single dose of 5-FU (150 mg/kg), and the kinetics of hematopoietic recovery was measured in the peripheral blood at the indicated time. Recovery of white blood cells (WBC) (A), platelets (B), and red blood cells (RBC) (C). Data are from 2 independent experiments (n = 8–10 mice, plotted as mean ± SD). (D). *Gpr56*-deficient mice exhibit normal sensitivity to repetitive myelosuppressive stress. Mice were injected intraperitoneally with 5-FU weekly for a total of 3 weeks, and survival was monitored daily. Survival data were analyzed using a log-rank non-parametric test (Mantel–Cox test), and shown as Kaplan–Meier survival curves (n = 12 animals per genotype over two independent experiments).

recovery kinetics and cell numbers between *Gpr56*-deficient mice and WT littermates. We next sought to determine the involvement of GPR56 signaling in HSC cell cycle regulation during myeloablative stress, as it has been reported that repetitive 5-FU treatment brings HSCs into continuous proliferation and ultimately leads to their exhaustion (Schepers et al., 2012). We treated mice with 5-FU (150 mg/kg, i.p.) once per week for a total of 3 weeks, and monitored the survival of mice daily; however, the median survival rates of *Gpr56*-deficient mice were not significantly different from WT

Figure 4 *Gpr56* deficiency does not impair HSC engraftment and multi-lineage repopulating activity in vivo. (A). Representative FACS plots show the distribution of cell cycle stages of BM HSPC subsets from WT or *Gpr56*-deficient mice. BM cells were first surface stained to define the HSPC subsets and further stained intracellularly for Ki-67 and Hoechst 33342. (B). The percentages of cells in each stage of cell cycle: G0 (Ki-67^{lo} Hoechst^{-}), G1 (Ki-67^{+} Hoechst^{-}), and S/G2/M (Ki-67^{+} Hoechst^{+}), are summarized in the graph. (n = 5 mice per genotype, mean ± SEM). (C). Apoptosis rates among BM LSK cells from WT or *Gpr56*-deficient mice as determined by Annexin V/7-AAD staining. Representative FACS plots show the percentages of apoptotic cells among LSK cells. The bar graph represents the percentages of early apoptotic cells (Annexin V^{+} 7-AAD^{-}) among LSK cells (n = 8 mice per genotype, mean ± SEM). (D). Schematic of serial competitive transplantation assay: Total BM cells from CD45.2^{+} WT or *Gpr56*-deficient mice were mixed with equal numbers of congenic (CD45.1^{+}) recipient-type BM cells (1:1) and competitively transplanted into lethally irradiated primary (CD45.1^{+}) recipient mice. After 20 weeks, total BM from primary recipients was transplanted into secondary recipients at 1 × 10^{6} cells per secondary recipient. (E–H). Donor chimerism (CD45.2^{+}) in primary recipient mice was determined by FACS analysis of peripheral blood. Bar graphs show the percentages of total donor cells (CD45.2^{+}) (E); donor B-cells (CD45.2^{+}B220^{+}) (F); donor myeloid cells (CD45.2^{+}CD11b^{+}Gr1^{+}) (G); and donor-T cells (CD45.1^{+} CD3^{+}) (H) at the indicated time points (n = 7–8 mice, mean ± SD). (I–J). At 20-weeks after transplantation, recipient BM was analyzed for total donor-derived cells (CD45.2^{+}) (I) and donor LSK frequency (J). (n = 7 mice, mean ± SD). (K–M). Analysis of secondary BM transplant recipients. Donor chimerism in peripheral blood at 4 and 12 weeks post-transplant (K). Total donor chimerism in BM (L). Percent donor-derived LSK cells in the BM at 12 weeks after secondary transplantation (n = 6 mice, mean ± SD) (M). *$p < 0.05$, **$p < 0.01$, and *n.s.* (not significant).

littermate controls (13 days vs. 16 days for *Gpr56*-deficient mice and WT mice, respectively; $p = 0.106$). (Fig. 5D). These data indicate that *Gpr56*-deficiency does not significantly affect hematopoietic regeneration during hematopoietic recovery from myeloablative stress.

Bone marrow HSPC retention and release are fine-tuned by the orchestrated action of molecular signals generated by cell-intrinsic and extrinsic cues within the BM microenvironment (Dar et al., 2006; Greenbaum and Link, 2011). GPR56 has been implicated in the regulation of migration and adhesion of neuronal progenitor cells and various malignant cells via $G\alpha_{12/13}$ and Rho GTPase signaling pathways (Iguchi et al., 2008; Shashidhar et al., 2005; Koirala et al., 2009). We therefore examined whether GPR56 might also be involved in the regulation of HSPC migration. To this end, we performed *in vitro* transwell migration assays to assess the ability of *Gpr56*-deficient HSPCs to migrate in response to a gradient of SDF-1α (Fig. 6A), a ligand for CXCR4 and a well-described

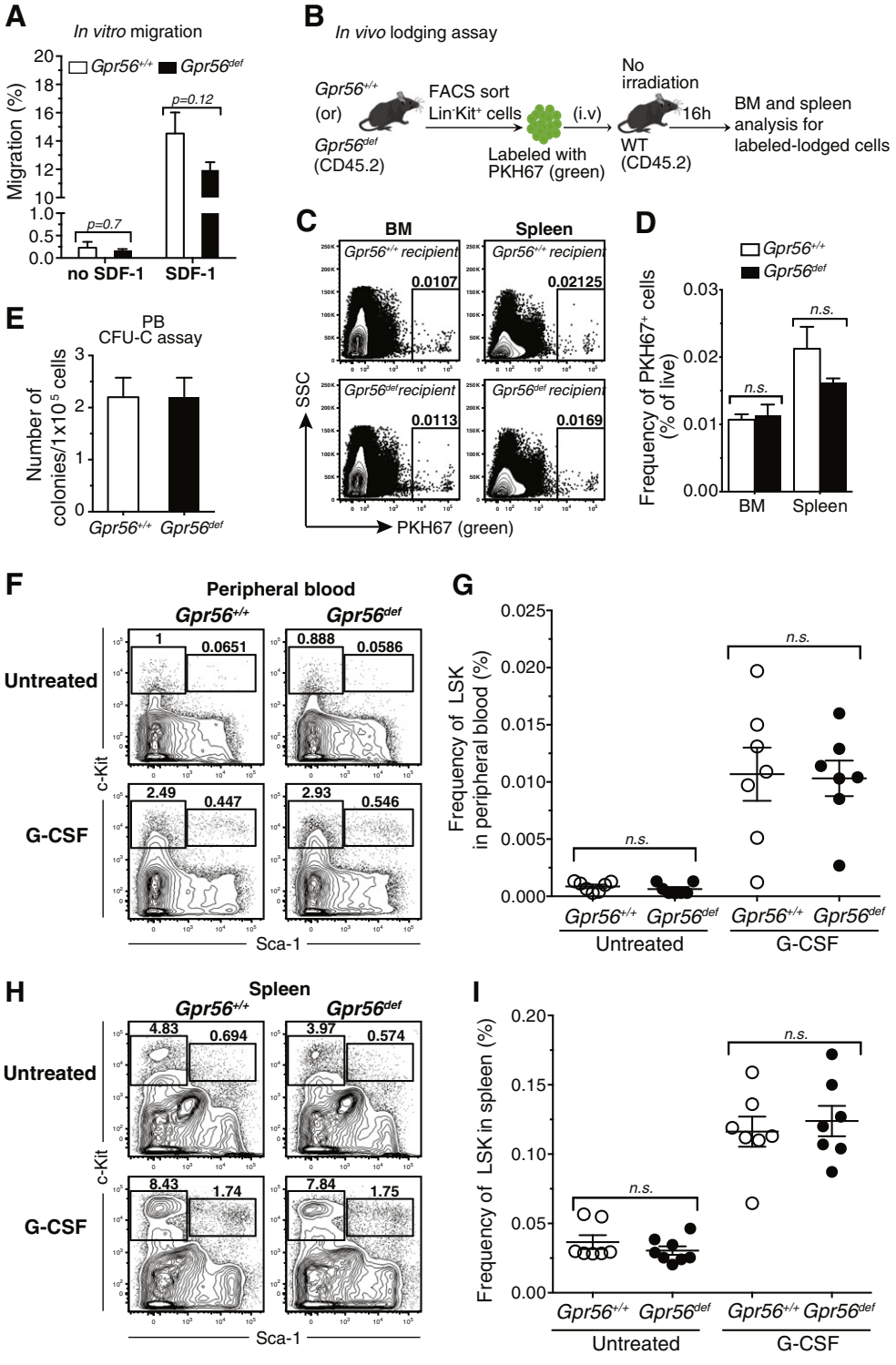

chemoattractant of HSPCs (Wright et al., 2002; Dar et al., 2006). Both WT and *Gpr56*-deficient HSPCs migrated well in response to SDF-1α, suggesting that *Gpr56*-deficiency on HSPCs does not impair their migratory capacity.

To directly assess the ability of HSPCs to interact with their niche in vivo, we next performed an *in vivo* lodgment assay in which an equal number of FACS-purified $Lin^{-}Kit^{+}$ cells (enriched for HSPCs) from WT or *Gpr56*-deficient mice BM were fluorescently labeled and transplanted intravenously into non-irradiated WT littermates (Luo et al., 2011b). Sixteen-hours post-transplantation, we assessed the frequency of cells within the BM and spleen (Figs. 6B–D). Labeled cells from *Gpr56*-deficient mice were lodged in the BM ($p = 0.74$) and spleen ($p = 0.17$) of recipient animals with similar frequency to their WT counterparts. We also analyzed HSPC frequencies in the peripheral blood (PB) and spleen in the steady-state using colony-forming assays and FACS. Both WT and *Gpr56*-deficient mice displayed similar HSPC content in PB and spleen (Figs. 6E–I), suggesting that GPR56 does not regulate bone marrow HSPC retention or trafficking under physiological conditions. Finally, to test the effect of *Gpr56*-deficiency on pharmacologically-induced HSPC mobilization, we treated mice with G-CSF for five days, a commonly used regimen in clinical settings to induce HSPC mobilization for transplantation therapies (Neben et al., 1993; Wright et al., 2002). Again, we saw no differences in circulating HSPC frequencies between G-CSF-treated WT and *Gpr56*-deficient mice (Figs. 6E–I). Collectively, these results suggest that reduction of *Gpr56* does not affect BM HSPC retention or release in the steady-state or in response to G-CSF-induced mobilization.

Discussion

In this study, we explored the expression pattern and functional significance of GPR56 in the regulation of hematopoietic stem and progenitor maintenance and function during steady-state and stress-induced hematopoiesis. We found that *Gpr56* is predominantly expressed in primitive HSPCs during embryonic definitive and adult hematopoiesis and is regulated in adult BM by core HSC transcription factors. Yet, despite its predominant expression in HSCs, high level *Gpr56* expression appears largely dispensable for HSC maintenance in the bone marrow of mice. While we were undertaking this study, Saito et al. (2013), reported that GPR56 signaling maintains HSC quiescence and retention in BM niches via regulation of apoptosis, cell cycle, adhesion, and migration through Rho-GTPase signaling, and in a Evi1-regulated manner (Saito et al., 2013). However, in our studies, we were unable to identify any differences in HSPC maintenance or differentiation capacity associated with the reduction of GPR56. Although the $Gpr56^{-/-}$ mice studied by Saito et al. (2013), and the *Gpr56*-deficient mice used in this study were generated by and obtained from the same source as that used in other studies of GPR56 function (Saito et al., 2013; Li et al., 2008; Koirala et al., 2009; Wu et al., 2013), all of the hematopoietic subsets we investigated, including phenotypic HSPCs and mature cell lineages in bone marrow, spleen, and blood were intact in the *Gpr56*-deficient mice, at least under the conditions tested here. There were, however, subtle phenotypes observed in our *Gpr56*-deficient mice, including an enlarged thymus, increased frequency of early thymic precursors and $CD4^{+}$ T cells, and lower percentages of $CD4^{+}$ and $CD8^{+}$ T cells among lymphocytes in the spleen suggesting a possible role for GPR56 in the regulation of mature T lymphopoiesis in the thymus. Increased ETP and DN2 frequency despite normal proliferation and survival suggests that in the steady state GPR56 signaling may negatively regulate the entry of progenitors into the thymus. Similar observations were reported for mice deficient for the transcription factor Egr1 (Schnell et al., 2006), although further studies will be required to unravel the cellular and molecular mechanisms through which GPR56 regulates thymus size.

Gpr56-deficient HSPCs displayed proliferation and apoptotic rates similar to that of WT HSPCs in vivo. Moreover, in contrast to previous studies (Saito et al., 2013), *Gpr56*-deficient HSPCs were able to regenerate the hematopoietic system normally in irradiated recipient mice in primary competitive BM transplantation settings. *Gpr56*-deficient HSPCs also displayed a normal pattern of hematopoietic recovery from myelosuppression after treatment with 5-FU in vivo, indicating that high levels of *Gpr56* expression are not required for the repopulating activity of HSCs in vivo, although the mild impairment of reconstituting activity seen upon serial transplant of *Gpr56*-deficient HSPCs suggests that sustained GPR56 activity may be important for maintaining hematopoietic function during prolonged hematopoietic stress. Our observations that HSPC numbers and functions remain intact in *Gpr56*-deficient mice despite disruption of both *Gpr56* alleles and substantial reduction of GPR56 protein is consistent with a recent report focused on stem cell function in skeletal muscle, which likewise found no significant muscle phenotypes in *Gpr56*-deficient animals or patients (Wu et al., 2013).

Figure 6 *Gpr56* deficiency does not affect the physiological or pharmacologically-induced migration of HSPCs. (A). In vitro migration of FACS isolated LSK cells from WT or *Gpr56*-deficient mice was assessed in Transwell migration assays. The percentage of migrated cells after 4 h was determined for spontaneous migration (no SDF-1α) or in response to chemotactic signals (toward 100 ng/ml of SDF-1α gradient). Cell migration was quantified by FACS analysis (n = 4 mice per experimental group, mean ± SD). (B). Schematic of in vivo lodging assay. (C). Representative FACS plots showing the percentages of labeled lodged cells ($PKH67^{+}$ cells, green) in the BM and spleen of recipient mice. (D). Bar graph summarizes the frequency of lodged cells among the live BM and spleen cells (n = 4 animals per group, mean ± SD. (E). Total number of colonies formed from PB cells (1×10^5) from WT or *Gpr56*-deficient mice (n = 4–5 per genotype) in methylcellulose based colony-forming unit (CFU) activity assay (mean ± SD. (F and H). FACS contour plots show the percentages of LSK and myeloid progenitor cells ($LS^{-}K^{+}$) among the Lin^{-} cells of peripheral blood (F), and spleen (H) from untreated (top) or G-CSF-treated (bottom) WT or *Gpr56*-deficient animals. Graphs show the frequencies of LSK cells in the peripheral blood (G), and spleen (I) from untreated and G-CSF treated WT and *Gpr56*-deficient mice. Data are plotted as mean ± SD, from two independent experiments (n = 7–8 animals per group).

G-protein coupled receptors are highly conserved across species and show structural homology with the other members of this family, and their mechanisms of action can be context-dependent and tissue specific (Venkatakrishnan et al., 2013; Wu et al., 2013; Kinzer-Ursem and Linderman, 2007). GPR56 signaling has been implicated in the regulation of neuronal progenitor cell adhesion and migration in the brain; however, we failed to detect such functions for GPR56 in HSPCs in the BM microenvironment, illuminating the tissue-specific, and context-dependent regulation of GPR56 signaling. The underlying basis for the distinct functions of GPR56 in the brain versus other tissue remains unclear. It is possible that closely related GPCR proteins or other unknown factors can compensate for reduced GPR56 in the adult hematopoietic, but not neural, progenitors. Potentially confounding compensatory signals arising from hematopoietic and non-hematopoietic cells (such as, HSPC niche components) in response to germline disruption of *Gpr56* and could also provide a selection advantage during homeostasis toward maintaining normal HSPC numbers in vivo. Finally, given our surprising observation that residual GPR56 protein can be detected using a mouse anti-human GPR56 monoclonal antibody in *Gpr56*-deficient mice, which previously have been reported to lack this protein entirely based on staining with a rabbit anti-human GPR56 antibody that was pre-cleared with mouse brain homogenates from GPR56 knockout mice, we cannot exclude the possibility that the residual protein expression we detect in these mice (Fig. 2B and Supplemental Figs. S2B–E) is sufficient to mediate the crucial functions of GPR56 in HSPCs, though perhaps not in other cell types. Furthermore, humans and mice harbor four splicing variants of *GPR56*, among which the S4 variant has its starting ATG in exon 4 of the gene (Kim et al., 2009). The targeting strategy used to generate the *Gpr56*-deficient mice used in this and prior studies (Luo et al., 2011a; Saito et al., 2013; Koirala et al., 2009; Wu et al., 2013) was designed to delete exons 2 and 3, and likely fails to delete the S4 variant. Thus, it is possible that the existing *Gpr56* knockout allele is actually a hypomorphic allele and that the generation of new targeting constructs that delete all forms of GPR56 will reveal a role for this protein in physiological processes that can proceed relatively normally with even very low levels of receptor. It is also possible that different levels of residual protein expression or different ratios of *GPR56* splice variants in $Gpr56^{-/-}$ mice housed in different animal facilities might ultimately provide an explanation for the different hematopoietic phenotypes observed in *Gpr56*-deficient mice in our studies and those of Saito et al. (2013), as a slightly higher level of residual GPR56 protein in our animals might be sufficient for GPR56 to perform its normal physiological functions. Such impacts of housing conditions on animal phenotype have been noted in other studies, which have further implicated differences in microbiome composition as a critical underlying variable (Kriegel et al., 2011). Further studies to identify GPR56 regulatory or compensatory signals and/or conditional deletion of *Gpr56* in specific hematopoietic lineages will be very helpful for further dissecting the activities of Gpr56 in physiological and regenerative hematopoiesis. In any event, our data clearly argue that high level Gpr56 expression is largely dispensable for adult hematopoietic stem and progenitor cell maintenance in the BM niche and regenerative functions in mice.

Summary

This work identifies the G-protein coupled receptor GPR56 as a cell surface protein that is expressed predominantly in long-term reconstituting hematopoietic stem and progenitor cells (HSPCs) in the adult bone marrow and regulated by a core set of hematopoietic transcription factors. However, despite enriched expression in HSPCs, reduced expression of GPR56 in gene-targeted *Gpr56*-deficient mice, revealed only subtle alterations in the hematopoietic compartment, with normal HSPC functions in both steady-state and regenerative hematopoiesis. Gpr56-deficiency also did not disrupt the physiological or pharmacologically-induced migration of HSPCs. These data suggest that high-level expression of GPR56 is dispensable for adult blood cell formation.

Acknowledgments

We thank all the members of Wagers laboratory and E. Gussoni and E. Dzierzak for helpful discussions. We also thank A. Wakabayashi, G. Buruzula and J. LaVecchio at Joslin/HSCI Flow Cytometry Core for excellent flow cytometry support, funded in part by NIH P30 DK036836. This work was supported in part by grants from the National Institutes of Health (NIH, OD004345 and HL088582 to AJW and DK67536 and DK103215 to RNK), from the National Health and Medical Research Council of Australia 1042934, 1024364 and 1008515 to JEP), and from Leukaemia and Lymphoma Research (LLR) grant 10015 to KO. Content is solely the responsibility of the authors and does not necessarily reflect the official views of the NIH or other funding agencies. The mouse strain used for this research project, B6N.129S5-*Gpr56*^{tm1Lex}/Mmcd, identification number 032342-UCD, was obtained from the Mutant Mouse Regional Resource Center, a NCRR–NIH funded strain repository, and was donated to the MMRRC by Genentech, Inc.

Appendix A. Supplementary data

Supplementary data to this article can be found online at http://dx.doi.org/10.1016/j.scr.2015.02.001.

References

Bagger, F.O., Rapin, N., Theilgaard-Monch, K., Kaczkowski, B., Jendholm, J., Winther, O., Porse, B., 2012. HemaExplorer: a web server for easy and fast visualization of gene expression in normal and malignant hematopoiesis. Blood 119 (26), 6394–6395. http://dx.doi.org/10.1182/blood-2012-05-427310 (Epub 2012/06/30. PubMed PMID: 22745298).

Beck, D., Thoms, J.A., Perera, D., Schutte, J., Unnikrishnan, A., Knezevic, K., Kinston, S.J., Wilson, N.K., O'Brien, T.A., Gottgens, B., Wong, J.W., Pimanda, J.E., 2013. Genome-wide analysis of transcriptional regulators in human HSPCs reveals a densely interconnected network of coding and noncoding genes. Blood 122 (14), e12–e22. http://dx.doi.org/10.1182/blood-2013-03-490425 (Epub 2013/08/27. PubMed PMID: 23974199).

Chambers, S.M., Boles, N.C., Lin, K.Y., Tierney, M.P., Bowman, T.V., Bradfute, S.B., Chen, A.J., Merchant, A.A., Sirin, O., Weksberg, D.C., Merchant, M.G., Fisk, C.J., Shaw, C.A., Goodell, M.A., 2007. Hematopoietic fingerprints: an expression database of stem cells and their progeny. Cell Stem Cell 1 (5), 578–591. http://dx.doi.org/10.1016/j.stem.2007.10.003 (Epub 2008/03/29. PubMed PMID: 18371395).

Dar, A., Kollet, O., Lapidot, T., 2006. Mutual, reciprocal SDF-1/CXCR4 interactions between hematopoietic and bone marrow stromal cells

regulate human stem cell migration and development in NOD/SCID chimeric mice. Exp. Hematol. 34 (8), 967–975. http://dx.doi.org/10.1016/j.exphem.2006.04.002 (Epub 2006/07/26, PubMed PMID: 16863903).

Ehninger, A., Trumpp, A., 2011. The bone marrow stem cell niche grows up: mesenchymal stem cells and macrophages move in. J. Exp. Med. 208 (3), 421–428.

Fitch, S.R., Kimber, G.M., Wilson, N.K., Parker, A., Mirshekar-Syahkal, B., Gottgens, B., Medvinsky, A., Dzierzak, E., Ottersbach, K., 2012. Signaling from the sympathetic nervous system regulates hematopoietic stem cell emergence during embryogenesis. Cell Stem Cell 11 (4), 554–566. http://dx.doi.org/10.1016/j.stem.2012.07.002 (Epub 2012/10/09. PubMed PMID: 23040481).

Forsberg, E.C., Passegue, E., Prohaska, S.S., Wagers, A.J., Koeva, M., Stuart, J.M., Weissman, I.L., 2010. Molecular signatures of quiescent, mobilized and leukemia-initiating hematopoietic stem cells. PLoS One 5 (1), e8785 (PubMed PMID: 20098702).

Gazit, R., Garrison, B.S., Rao, T.N., Shay, T., Costello, J., Ericson, J., Kim, F., Collins, J.J., Regev, A., Wagers, A.J., Rossi, D.J., 2013. Transcriptome analysis identifies regulators of hematopoietic stem and progenitor cells. Stem Cell Rep. 1 (3), 266–280. http://dx.doi.org/10.1016/j.stemcr.2013.07.004 (Epub 2013/12/10. PubMed PMID: 24319662; PubMed Central PMCID: PMC3849420).

Greenbaum, A.M., Link, D.C., 2011. Mechanisms of G-CSF-mediated hematopoietic stem and progenitor mobilization. Leukemia 25 (2), 211–217. http://dx.doi.org/10.1038/leu.2010.248 (Epub 2010/11/17, PubMed PMID: 21079612).

Iguchi, T., Sakata, K., Yoshizaki, K., Tago, K., Mizuno, N., Itoh, H., 2008. Orphan G protein-coupled receptor GPR56 regulates neural progenitor cell migration via a G alpha 12/13 and Rho pathway. J. Biol. Chem. 283 (21), 14469–14478. http://dx.doi.org/10.1074/jbc.M708919200 (Epub 2008/04/02. PubMed PMID: 18378689).

Ivanova, N.B., Dimos, J.T., Schaniel, C., Hackney, J.A., Moore, K.A., Lemischka, I.R., 2002. A stem cell molecular signature. Science 298 (5593), 601–604 (PubMed PMID: 12228721).

Jeong, S.J., Luo, R., Li, S., Strokes, N., Piao, X., 2012. Characterization of G protein-coupled receptor 56 protein expression in the mouse developing neocortex. J. Comp. Neurol. 520 (13), 2930–2940. http://dx.doi.org/10.1002/cne.23076 (Epub 2012/02/22. PubMed PMID: 22351047).

Kiel, M.J., Yilmaz, O.H., Iwashita, T., Terhorst, C., Morrison, S.J., 2005. SLAM family receptors distinguish hematopoietic stem and progenitor cells and reveal endothelial niches for stem cells. Cell 121 (7), 1109–1121 (PubMed PMID: 15989959).

Kim, Y.J., Huh, J.W., Kim, D.S., Bae, M.I., Lee, J.R., Ha, H.S., Ahn, K., Kim, T.O., Song, G.A., Kim, H.S., 2009. Molecular characterization of the DYX1C1 gene and its application as a cancer biomarker. J. Cancer Res. Clin. Oncol. 135 (2), 265–270. http://dx.doi.org/10.1007/s00432-008-0445-8 (Epub 2008/07/12, PubMed PMID: 18618141).

Kinzer-Ursem, T.L., Linderman, J.J., 2007. Both ligand- and cell-specific parameters control ligand agonism in a kinetic model of g protein-coupled receptor signaling. PLoS Comput. Biol. 3 (1), e6. http://dx.doi.org/10.1371/journal.pcbi.0030006 (Epub 2007/01/16, PubMed PMID: 17222056).

Koirala, S., Jin, Z., Piao, X., Corfas, G., 2009. GPR56-regulated granule cell adhesion is essential for rostral cerebellar development. J. Neurosci. Off. J. Soc. Neurosci. 29 (23), 7439–7449. http://dx.doi.org/10.1523/JNEUROSCI.1182-09.2009 (Epub 2009/06/12. PubMed PMID: 19515912).

Kriegel, M.A., Sefik, E., Hill, J.A., Wu, H.J., Benoist, C., Mathis, D., 2011. Naturally transmitted segmented filamentous bacteria segregate with diabetes protection in nonobese diabetic mice. Proc. Natl. Acad. Sci. U. S. A. 108 (28), 11548–11553. http://dx.doi.org/10.1073/pnas.1108924108 (PubMed PMID: 21709219).

Laird, D.J., von Andrian, U.H., Wagers, A.J., 2008. Stem cell trafficking in tissue development, growth, and disease. Cell 132 (4), 612–630 (PubMed PMID: 18295579).

Langenhan, T., Aust, G., Hamann, J., 2013. Sticky signaling–adhesion class G protein-coupled receptors take the stage. Sci. Signal. 6 (276), re3. http://dx.doi.org/10.1126/scisignal.2003825 (Epub 2013/05/23. PubMed PMID: 23695165).

Levesque, J.P., Winkler, I.G., 2011. Hierarchy of immature hematopoietic cells related to blood flow and niche. Curr. Opin. Hematol. 18 (4), 220–225. http://dx.doi.org/10.1097/MOH.0b013e3283475fe7 (Epub 2011/04/27. PubMed PMID: 21519242).

Li, S., Jin, Z., Koirala, S., Bu, L., Xu, L., Hynes, R.O., Walsh, C.A., Corfas, G., Piao, X., 2008. GPR56 regulates pial basement membrane integrity and cortical lamination. J. Neurosci. Off. J. Soc. Neurosci. 28 (22), 5817–5826. http://dx.doi.org/10.1523/JNEUROSCI.0853-08.2008 (Epub 2008/05/30. PubMed PMID: 18509043).

Ling, K.W., Ottersbach, K., van Hamburg, J.P., Oziemlak, A., Tsai, F.Y., Orkin, S.H., Ploemacher, R., Hendriks, R.W., Dzierzak, E., 2004. GATA-2 plays two functionally distinct roles during the ontogeny of hematopoietic stem cells. J. Exp. Med. 200 (7), 871–882 (PubMed PMID: 15466621).

Luo, R., Jeong, S.J., Jin, Z., Strokes, N., Li, S., Piao, X., 2011a. G protein-coupled receptor 56 and collagen III, a receptor–ligand pair, regulates cortical development and lamination. Proc. Natl. Acad. Sci. U. S. A. 108 (31), 12925–12930. http://dx.doi.org/10.1073/pnas.1104821108 (Epub 2011/07/20. PubMed PMID: 21768377).

Luo, B., Lam, B.S., Lee, S.H., Wey, S., Zhou, H., Wang, M., Chen, S.Y., Adams, G.B., Lee, A.S., 2011b. The endoplasmic reticulum chaperone protein GRP94 is required for maintaining hematopoietic stem cell interactions with the adult bone marrow niche. PLoS One 6 (5), e20364. http://dx.doi.org/10.1371/journal.pone.0020364 (Epub 2011/06/08, PONE-D-11-02406 [pii]. PubMed PMID: 21647226).

Neben, S., Marcus, K., Mauch, P., 1993. Mobilization of hematopoietic stem and progenitor cell subpopulations from the marrow to the blood of mice following cyclophosphamide and/or granulocyte colony-stimulating factor. Blood 81 (7), 1960–1967 (PubMed PMID: 7681707).

Orkin, S.H., Zon, L.I., 2008. Hematopoiesis: an evolving paradigm for stem cell biology. Cell 132 (4), 631–644 (PubMed PMID: 18295580).

Passegue, E., Wagers, A.J., Giuriato, S., Anderson, W.C., Weissman, I.L., 2005. Global analysis of proliferation and cell cycle gene expression in the regulation of hematopoietic stem and progenitor cell fates. J. Exp. Med. 202 (11), 1599–1611 (PubMed PMID: 16330818).

Piao, X., Hill, R.S., Bodell, A., Chang, B.S., Basel-Vanagaite, L., Straussberg, R., Dobyns, W.B., Qasrawi, B., Winter, R.M., Innes, A.M., Voit, T., Ross, M.E., Michaud, J.L., Descarie, J.C., Barkovich, A.J., Walsh, C.A., 2004. G protein-coupled receptor-dependent development of human frontal cortex. Science 303 (5666), 2033–2036. http://dx.doi.org/10.1126/science.1092780 (Epub 2004/03/27. PubMed PMID: 15044805).

Ramalho-Santos, M., Yoon, S., Matsuzaki, Y., Mulligan, R.C., Melton, D.A., 2002. "Stemness": transcriptional profiling of embryonic and adult stem cells. Science 298 (5593), 597–600 (PubMed PMID: 12228720).

Riddell, J., Gazit, R., Garrison, B.S., Guo, G., Saadatpour, A., Mandal, P.K., Ebina, W., Volchkov, P., Yuan, G.C., Orkin, S.H., Rossi, D.J., 2014. Reprogramming committed murine blood cells to induced hematopoietic stem cells with defined factors. Cell 157 (3), 549–564. http://dx.doi.org/10.1016/j.cell.2014.04.006 (Epub 2014/04/29. PubMed PMID: 24766805).

Saito, Y., Kaneda, K., Suekane, A., Ichihara, E., Nakahata, S., Yamakawa, N., Nagai, K., Mizuno, N., Kogawa, K., Miura, I., Itoh, H., Morishita, K., 2013. Maintenance of the hematopoietic stem cell pool in bone marrow niches by EVI1-regulated GPR56. Leukemia 27 (8), 1637–1649. http://dx.doi.org/10.1038/leu.2013.75 (Epub 2013/03/13. PubMed PMID: 23478665).

Schepers, K., Hsiao, E.C., Garg, T., Scott, M.J., Passegue, E., 2012. Activated Gs signaling in osteoblastic cells alters the hematopoietic stem cell niche in mice. Blood 120 (17), 3425–3435. http://dx.doi.org/10.1182/blood-2011-11-395418 (Epub 2012/08/04. PubMed PMID: 22859604).

Schnell, F.J., Zoller, A.L., Patel, S.R., Williams, I.R., Kersh, G.J., 2006. Early growth response gene 1 provides negative feedback to inhibit entry of progenitor cells into the thymus. J. Immunol. 176 (8), 4740–4747 (Epub 2006/04/06. PubMed PMID: 16585567).

Shashidhar, S., Lorente, G., Nagavarapu, U., Nelson, A., Kuo, J., Cummins, J., Nikolich, K., Urfer, R., Foehr, E.D., 2005. GPR56 is a GPCR that is overexpressed in gliomas and functions in tumor cell adhesion. Oncogene 24 (10), 1673–1682. http://dx.doi.org/10.1038/sj.onc.1208395 (Epub 2005/01/28. PubMed PMID: 15674329).

Solaimani Kartalaei, P., Yamada-Inagawa, T., Vink, C.S., de Pater, E., van der Linden, R., Marks-Bluth, J., van der Sloot, A., van den Hout, M., Yokomizo, T., van Schaick-Solerno, M.L., Delwel, R., Pimanda, J.E., van, I.W.F., Dzierzak, E., 2015. Whole-transcriptome analysis of endothelial to hematopoietic stem cell transition reveals a requirement for Gpr56 in HSC generation. J. Exp. Med. 212 (1), 93–106. http://dx.doi.org/10.1084/jem.20140767 PubMed PMID: 25547674).

Venezia, T.A., Merchant, A.A., Ramos, C.A., Whitehouse, N.L., Young, A.S., Shaw, C.A., Goodell, M.A., 2004. Molecular signatures of proliferation and quiescence in hematopoietic stem cells. PLoS Biol. 2 (10), e301 (PubMed PMID: 15459755).

Venkatakrishnan, A.J., Deupi, X., Lebon, G., Tate, C.G., Schertler, G.F., Babu, M.M., 2013. Molecular signatures of G-protein-coupled receptors. Nature 494 (7436), 185–194. http://dx.doi.org/10.1038/nature11896 (Epub 2013/02/15. PubMed PMID: 23407534).

Wang, L.D., Wagers, A.J., 2011. Dynamic niches in the origination and differentiation of haematopoietic stem cells. Nat. Rev. Mol. Cell Biol. 12 (10), 643–655. http://dx.doi.org/10.1038/nrm3184 (Epub 2011/09/03. nrm3184 [pii]. PubMed PMID: 21886187).

Wilson, N.K., Foster, S.D., Wang, X., Knezevic, K., Schutte, J., Kaimakis, P., Chilarska, P.M., Kinston, S., Ouwehand, W.H., Dzierzak, E., Pimanda, J.E., de Bruijn, M.F., Gottgens, B., 2010. Combinatorial transcriptional control in blood stem/progenitor cells: genome-wide analysis of ten major transcriptional regulators. Cell Stem Cell 7 (4), 532–544. http://dx.doi.org/10.1016/j.stem.2010.07.016 (Epub 2010/10/05. PubMed PMID: 20887958).

Wright, D.E., Bowman, E.P., Wagers, A.J., Butcher, E.C., Weissman, I.L., 2002. Hematopoietic stem cells are uniquely selective in their migratory response to chemokines. J. Exp. Med. 195 (9), 1145–1154 (PubMed PMID: 11994419).

Wu, M.P., Doyle, J.R., Barry, B., Beauvais, A., Rozkalne, A., Piao, X., Lawlor, M.W., Kopin, A.S., Walsh, C.A., Gussoni, E., 2013. G-protein coupled receptor 56 promotes myoblast fusion through serum response factor- and nuclear factor of activated T-cell-mediated signalling but is not essential for muscle development in vivo. FEBS J. 280 (23), 6097–6113. http://dx.doi.org/10.1111/febs.12529 (Epub 2013/10/10. PubMed PMID: 24102982).